Vortex Pinning and Dynamics in the Neutron Star Crust

Gabriel Wlazłowski,[1,2,*] Kazuyuki Sekizawa,[1,†] Piotr Magierski,[1,2,‡] Aurel Bulgac,[2,§] and Michael McNeil Forbes[3,2,‖]
[1]Faculty of Physics, Warsaw University of Technology, Ulica Koszykowa 75, 00–662 Warsaw, POLAND
[2]Department of Physics, University of Washington, Seattle, Washington 98195–1560, USA
[3]Department of Physics and Astronomy, Washington State University, Pullman, Washington 98164–2814, USA
(Received 10 June 2016; revised manuscript received 8 September 2016; published 30 November 2016)

The nature of the interaction between superfluid vortices and the neutron star crust, conjectured by Anderson and Itoh in 1975 to be at the heart vortex creep and the cause of glitches, has been a long-standing question in astrophysics. Using a qualitatively new approach, we follow the dynamics as superfluid vortices move in response to the presence of "nuclei" (nuclear defects in the crust). The resulting motion is perpendicular to the force, similar to the motion of a spinning top when pushed. We show that nuclei repel vortices in the neutron star crust, and characterize the force per unit length of the vortex line as a function of the vortex element to the nucleus separation.

DOI: 10.1103/PhysRevLett.117.232701

Introduction.—Pulsar glitches, sudden increases in the pulsation frequency, first observed in 1969 [1,2], provide one of the few observable probes into the interior of neutron stars [3]. Although many models have been proposed, the origin of large glitches remains a mystery. The current picture, proposed in 1975 by Anderson and Itoh [4], is that the quantized vortices in the superfluid interior of a neutron star store a significant amount of angular momentum. As these vortices "creep" through the crust, they transfer this angular momentum to the crust. Glitches result from a catastrophic release of pinned vorticity [5] that suddenly changes the pulsation rate.

This scenario involves two critical ingredients: the trigger mechanism for the catastrophic release (not considered here) and the vortex-"nucleus" interaction. (By nucleus we mean nucleilike objects embedded in a neutron superfluid as is expected in the crust of neutron stars.) The interaction can, in principle, be derived from a microscopic theory. However, despite considerable theoretical effort, even its sign remains uncertain. Until now, the force was evaluated by comparing (free) energies extracted from different static calculations: a vortex passing through a nucleus, a vortex and nucleus separated by an infinite distance, or an interstitial vortex between two neighboring nuclei [6–12]. As pointed out in Ref. [13], this approach only computes the pinning energy, and is not able to extract the full information about the vortex-nucleus interaction.

Despite these efforts, there is still no agreement about whether pinned or unpinned configurations are preferred. The problem is that subtracting two large energies arising from many contributions, typically of order 10^4 MeV, results in a tiny difference of order 1 MeV. Symmetry-unrestricted calculations are challenging, and only by imposing axial symmetry has the required 1 MeV accuracy been achieved [12,14]. Moreover, the difference is extremely sensitive to quantum shell effects that are not present in semiclassical simulations [6–9] and is sensitive to the particle number or background density which varies from one configuration to the next. (See [12] for extensive discussion.)

Here, we show that nuclei repel superfluid vortices and characterize the vortex-nucleus interaction within dynamical simulations as suggested in [15]. The sign of the force can be unambiguously determined by looking at the vortex motion (see the movie demonstrating the response of classical gyroscope when pushed in the Supplemental Material [16]). In 3D dynamical simulations, all relevant degrees of freedom of the vortex-nucleus system are active, and the behavior provides valuable insight for building effective theories of the vortex-nucleus system. Following [26], an effective hydrodynamic description can be formulated (see, also, [27–30])

$$T\frac{\partial^2 \boldsymbol{r}}{\partial z^2} + \rho_s \boldsymbol{\kappa} \times \left(\frac{\partial \boldsymbol{r}}{\partial t} - \boldsymbol{v}_s\right) + \boldsymbol{f}_{\mathrm{VN}} = 0, \tag{1}$$

where $\boldsymbol{r}$ is the position of the vortex core. The first term is tension force as the vortex is bent, characterized by coefficient T. The second term corresponds to Magnus force where $\boldsymbol{\kappa} = 2\pi\hbar\hat{\boldsymbol{l}}/2m_n$ is the circulation which points along the vortex, $\rho_s = m_n n$ is mass density while n is number density of superfluid neutron background, m_n is neutron mass, and $\boldsymbol{v}_s$ is the velocity of any ambient flow in the background superfluid density. The last contribution $\boldsymbol{f}_{\mathrm{VN}}$ defines the vortex-nucleus (VN) interaction in terms of the force per unit length. Clearly, the pinning energy alone does not provide sufficient information to describe the motion. In addition, all existing calculations assume that the vortices form straight lines and, thus, do not reveal information about the tension. It is demonstrated in [26] that pinning occurs irrespective of the sign of the vortex-nucleus interaction when $v_s < v_c \sim s^{1/2} F_m/\rho_s \kappa a$, where F_m is set by maximum magnitude of $\boldsymbol{f}_{\mathrm{VN}}$, $s = F_m/T$, and a is set by range of vortex-nucleus interaction. In this Letter,

we extract all effective quantities directly from a microscopic theory.

Method.—The most accurate and flexible microscopic approach to superfluid dynamics in nuclear systems is density functional theory (DFT), which, in principle, is an exact approach. Here, we use an extension of Kohn-Sham DFT known as the time-dependent superfluid local density approximation (TDSLDA), an orbital-based fermionic DFT that has been proven to be very accurate for describing the dynamics of strongly correlated fermionic systems in both ultracold atomic gases [31–37] and in nuclear systems [38–41]. In this approach, densities and the superfluid order parameter Δ are constructed from quasiparticle orbitals which are represented on a 3D lattice (without any symmetry restrictions) of size $75 \times 75 \times 60$ fm with lattice spacing corresponding to quite a large momentum cutoff $p_c \approx 400$ MeV$/c$, and a volume that is sufficient to fit a single nucleus and a quantum vortex with reasonable separation between the two. To prevent vortices from neighboring cells from interacting (due to the periodic boundary conditions), we introduce a flat-bottomed external potential confining the system in a tube of a radius 30 fm. (See [16] and [14] for details.) For initial states in our time-dependent simulations, we chose stationary self-consistent solutions of the TDSLDA with two constraints: (i) the center of mass of the protons is fixed at a specified position, (ii) the phase of the neutron pairing potential increases by 2π when moving around the center of the tube, i.e., $\Delta(\rho,z,\phi)=|\Delta(\rho,z)|\exp(i\phi)$, where $\rho=\sqrt{x^2+y^2}$ is the distance from the center of the tube and $\phi = \text{atan}(y/x)$. We produce initial states for two background neutron densities, $n = 0.014$ fm^{-3} and $n = 0.031$ fm^{-3}, with proton number $Z = 50$. These represent the zones 3 and 4 expected in neutron star crusts according to the classification of Negele and Vautherin [42]. Previous calculations are in clear disagreement in this region of densities. We start the simulations from two configurations: an unpinned configuration where the nucleus is located outside the vortex, close to the tube boundary, and a pinned configuration where the nucleus is located inside the vortex (see [16] for figures of these states).

The physics contained in the DFT is defined by the energy density functional $\mathcal{E}$ which is a functional of the single-particle orbitals. For the normal part, we use the FaNDF^0 functional constructed by Fayans *et al.* [43,44]. It reproduces the infinite matter equation of state of Refs. [45,46], many properties of nuclei [47,48], and allows one to construct a very efficient solver of the TDSLDA equations (see [16]). The only simplification we make is to omit the spin-orbit coupling term from the functional as this greatly reduces the computational cost. While the spin-orbit term is important for finite nuclei, in the present context, it is not expected to significantly impact the final results. The spin-orbit term does not affect uniform matter; thus, in our case, where the nuclei are embedded in a uniform gas of neutrons, it would shift the single-particle levels in the nucleus in such a way as not to influence the physics of the vortex-nucleus system, as shown in [12]. These hardly influence the physics of the vortex-nucleus system. Likewise, since the depletion of the normal density in the vortex core is small [49], the vortex density is approximately uniform and one expects the influence of the spin-orbit term on the structure of the vortex to be small. To the FaNDF^0 functional we add a contribution describing the pairing correlations, $\mathcal{E}_{\text{pair}}(\boldsymbol{r}) = g[n(\boldsymbol{r})]|\nu_n(\boldsymbol{r})|^2 + g[p(\boldsymbol{r})]|\nu_p(\boldsymbol{r})|^2$, where $\nu_{p,n}$ are the $S = 0$ proton and neutron anomalous densities (proportional to the pairing gaps $\Delta_{n,p}$), g is a density dependent coupling constant, and n/p is the density of neutrons or protons. The coupling constant g is chosen so as to reproduce the neutron pairing gap in pure neutron matter. It has the density dependence as predicted by BCS theory, but with maximum paring gap of 2 MeV (the full form is shown in [16]). The local portion of the anomalous densities $\nu_{n,p}$ diverges and requires regularization. We use the procedure described in Refs [50,51], the accuracy of which has been validated against a wide range of experimental results for cold atoms [31,32,34–37,52–54] and nuclear problems [38,40,47,49].

The TDSLDA approach automatically includes various dissipative processes, including superfluid and normal phonon excitations, Cooper pair breaking, and Landau damping. These are crucial for a correct description of vortex pinning and unpinning [55]. Consider pinning: for a nucleus to capture a vortex, the vortex must dissipate its collective energy, otherwise, it will simply orbit the nucleus as governed by the Magnus force, like a precessing spinning top. We demonstrated, in [37], that the TDSLDA accurately models the formation and decay of solitonic defects—from domain walls into vortex rings and vortex lines. These effects cannot be reproduced without dissipation, and the agreement with experiments [56,57] validates that the so-called one-body dissipation naturally present in the TDSLDA is sufficient to correctly capture vortex dynamics. With the TDSLDA approach, we can, thus, extract both the magnitude of the vortex-nucleus interaction as well as the dynamical time scales.

To extract the effective force between a quantized vortex and a nucleus, we apply Newton's laws. Suppose that only two forces act on the nucleus: the force $\boldsymbol{F}$ arising from the interaction with the vortex and a known external force $\boldsymbol{F}_{\text{ext}}$. In the simplest case, the vortex-nucleus force depends on the relative distance between interacting objects R. If the nucleus moves with a constant velocity $\boldsymbol{v}_0$ which is below the critical velocity (so that phonons are not excited), then the relation $\boldsymbol{F}(t) = -\boldsymbol{F}_{\text{ext}}(t)$ holds. Combining this information with the relative distance $R(t)$, we can extract the vortex-nucleus force as a function of the separation $\boldsymbol{F}(R)$, see Fig. 1. We choose the external force to be constant in space and acting only on the protons. This force moves the center of mass of the protons together with those neutrons bound (entrained) in the nucleus without

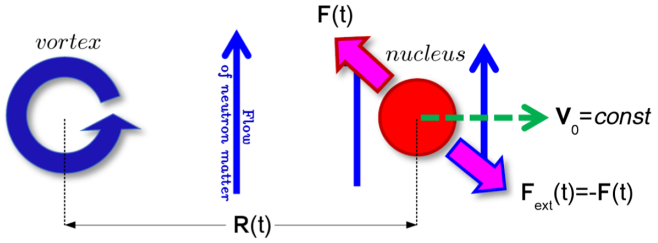

FIG. 1. Schematic figure explaining the method used for the force extraction. The force $\boldsymbol{F}$ depends on relative distance between vortex and nucleus R, moving with a constant velocity $\boldsymbol{v}_0$. The external force $\boldsymbol{F}_{\rm ext}(t)$ is chosen to compensate exactly $\boldsymbol{F}$.

significantly modifying the internal structure of the nucleus or surrounding neutron medium. We adjust the force to ensure that the center of mass of the protons moves with constant velocity $\boldsymbol{v}_0$

$$\boldsymbol{F}_{\rm ext}(t+\Delta t) = \boldsymbol{F}_{\rm ext}(t) - \alpha[\boldsymbol{v}(t) - \boldsymbol{v}_0], \tag{2}$$

where $\boldsymbol{v}(t)$ is the velocity of the center of mass of protons and α is the coefficient governing the rate of adjusting the force. In our simulations, we dragged the nucleus with a very small velocity $v_0 = 0.001c$ along the x axis to ensure that no phonons are excited. The velocity is far below the critical velocity of the system and is sufficiently small that the systems follow an almost adiabatic path.

Results of dynamical simulations.—In the first set of simulations, we start from an unpinned configuration and drag the nucleus towards the vortex. Figure 2 shows the time evolution of these systems for small vortex-nucleus separations (see [16] for movies of the entire simulations). As the nucleus approaches to the vortex, it exerts a force $\boldsymbol{F}(R)$ on the vortex which responds by moving according to the Magnus relationship $\boldsymbol{F}_M \propto \boldsymbol{\kappa} \times (\partial \boldsymbol{r}/\partial t)$, where $\boldsymbol{r}$ specifies the vortex-core position. The vortex is initially moving perpendicular to this force along the positive y direction visually confirming that the force is, indeed, repulsive and initially directed along the x axis away from the nucleus. In the case of attraction, the vortex would initially move along the negative y direction. For both densities considered, the vortex-nucleus interaction is clearly repulsive and increasing with density, a result in agreement with the hydrodynamic approximation [16]. The curvature of the vortex bending for the closest vortex-nucleus configuration is set by the nucleus. (There is also a small displacement of both ends of the vortex during the evolution in our simulation box.) For the higher density, the vortex induces visible nuclear prolate deformation with the elongation axis set by the vortex axis. To confirm the repulsive nature of the force at very small vortex-nucleus separations, we also start simulations from "pinned" configurations. In both cases, the vortex rapidly unpins (with a timescale shorter than 1000 fm/c); i.e., the vortex is immediately expelled from the nucleus, indicating that the pinned configuration is dynamically unstable. The initial

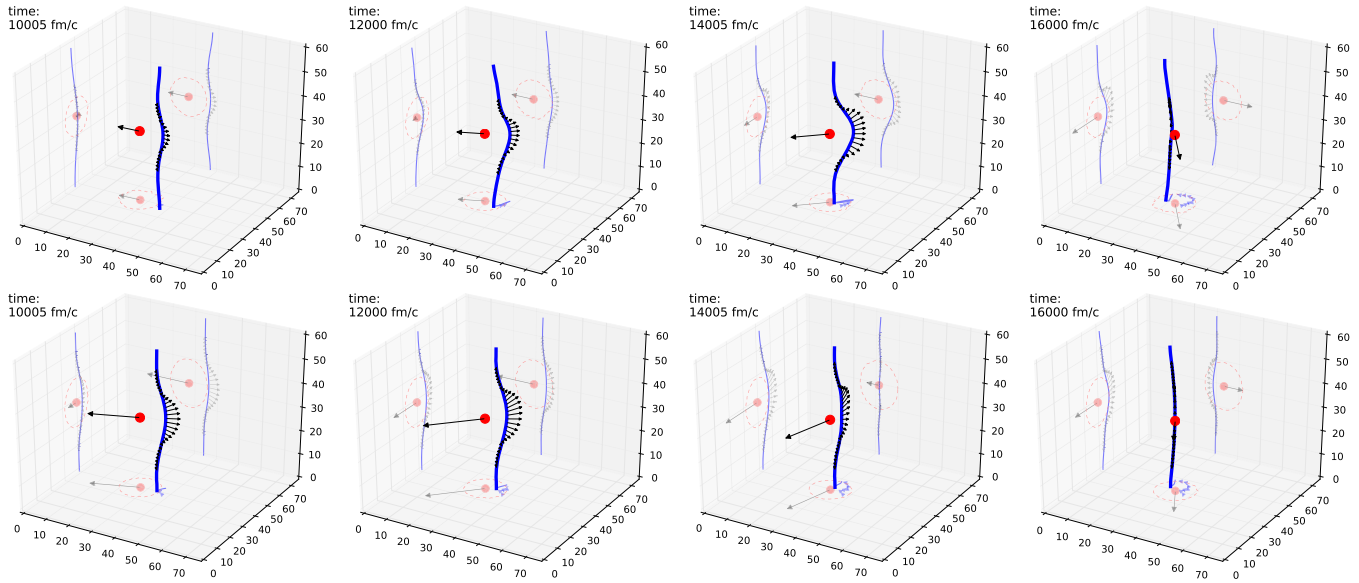

FIG. 2. Dynamics of the system for times corresponding to small vortex-nucleus separations for neutron matter density $n = 0.014$ fm^{-3} (top) and 0.031 fm^{-3} (bottom). Frames from left to right correspond to times $(10, 12, 14, 16) \times 1000$ fm/c (for full movies, see [16]). Blue line indicates the vortex core position extracted from the order parameter Δ (see [16] for details). Red dot indicates position of the center of mass of protons. The vector attached to the red dot denotes the vortex-nucleus force $\boldsymbol{F}(R)$. Vectors attached to the vortex indicate contributions to the force $-d\boldsymbol{F}$ extracted from force per unit length, see Eq. (3) and inset (a) of Fig. 3. They are scaled by a factor of 3 for better visibility. Projections of the view are shown on sides of the box. Red dashed lines denote shape of nucleus (defined as a point where density of protons drops to value 0.005 fm^{-3}). By blue triangles (on XY plane), trajectory of the vortex up to given time is shown.

energy is transferred into stretching of the vortex line as it bows out away from the nucleus.

Now, we will proceed to estimate the vortex tension T. The vortex is the longest at $t_{\max} \approx 14000$ fm$/c$ for both low and high densities, 0.014 fm^{-3} and 0.031 fm^{-3}, respectively. The length of the vortex increases by $\Delta L = L(t_{\max}) - L(0) = 3.5$ and 1.5 fm and the total excitation energy of the system is $E^* = E(t_{\max}) - E(0) = 5$ and 11 MeV, respectively. Assuming all of this energy is stored in the vortex, we obtain an upper bound on the vortex tension of $T \lesssim 1.4$ and 7.3 MeV/fm, respectively. The energy of a vortex line in the leading order hydrodynamic approximation is $E \approx \rho_s \kappa^2 L \ln(D/2\xi)/4\pi$ [16], where D is the diameter of the simulation cell, which has to be replaced with the average vortex separation l_v in the neutron star crust [58]. This simple hydrodynamic approximation suggests that different tensions arise from changes in the neutron superfluid density ρ_s and vortex core size ξ. Estimating $\rho_s \sim n$ gives a ratio of 0.77 [10], which is much larger than the ratio $1.4/7.3 \approx 0.18$ obtained from our microscopic simulations. At higher densities the vortex is, thus, much stiffer then expected from hydrodynamic estimates.

Force per unit vortex length.—Combining the information about the force $\boldsymbol{F}(t)$ with the vortex-nucleus separation $R(t)$, we extract the force for various separations R, defined as the distance within the plane perpendicular to the symmetry axis of the confining tube. We decompose the force into a tangential and a centripetal component with respect to the vortex position at each time. These results are presented in inset (b) of Fig. 3. The extracted force is predominantly central with a negligible tangential component. The effective range of the force is about 10 fm for the lower density, increasing to about 15 fm for the higher density, consistent with an increasing coherence length ξ with density and decreasing neutron pairing gap. The behavior of the total force for small separations demonstrates that it is not merely a function of a distance. At small separations, the deformation of the vortex line and the nuclear deformation become important degrees of freedom.

To characterize the effects of the vortex geometry, we extract the force per unit length $f(r)$. Inspired by the vortex filament model (see [59,60] and references therein), we divide the vortex line into elements of length $d\boldsymbol{l}$. Each element exerts force on a nucleus

$$d\boldsymbol{F} = f(r) \sin\alpha \hat{\boldsymbol{r}} dl, \tag{3}$$

where $\boldsymbol{r}$ denotes the position of the vortex line element from the center of mass of the protons, α is angle between vectors $d\boldsymbol{l}$ and $\boldsymbol{r}$ [see inset (a) of Fig. 3], and $\hat{\boldsymbol{r}} = \boldsymbol{r}/r$. The force $\boldsymbol{f}_{\rm VN}$ in Eq. (1) is given by $-f(r)\sin\alpha\hat{\boldsymbol{r}}$. The total force is the sum of contributions from all vortex elements $\boldsymbol{F} = \int_L d\boldsymbol{F}$. We model $f(r)$ with a Padé approximant with the asymptotic behavior $f(r \to \infty) \propto r^{-3}$ consistent with hydrodynamic predictions. The parameters of the Padé approximant are determined from a least-squares fit to all simulation data

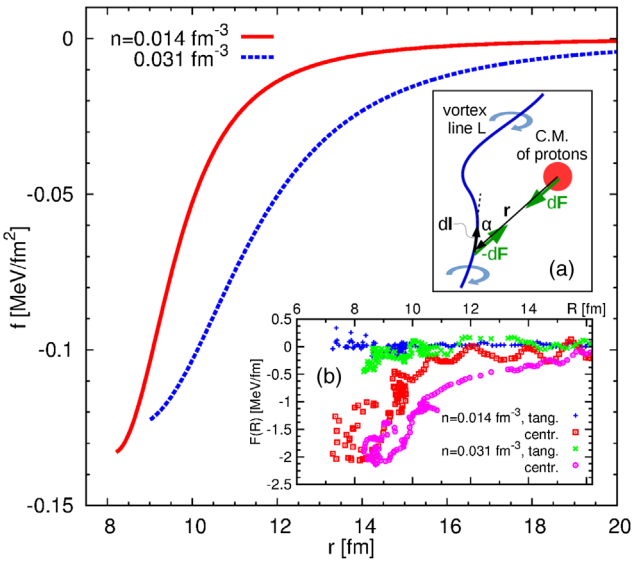

FIG. 3. Extracted force per unit length $f(r)$ for both densities. Negative values correspond to the repulsive force. In inset (a), the schematic configuration is shown explaining the extraction procedure according to Eq. (3). Inset (b) shows the measured total force $F(R)$ as shown in Fig. 1 for both densities. The force has been decomposed into tangential and centripetal components with respect to the instantaneous vortex position.

resulting in the force per unit length $f(r)$ characterization of the vortex-nucleus interaction shown in Fig. 3. (The hydrodynamic results and fitting procedure are described in detail in [16]). This simple characterization of the force $\boldsymbol{F}$ works better at lower densities, which is consistent with the larger nuclear deformations seen at higher densities. Nuclear deformations introduce an orientation dependence to the force that is not captured by the simple model (3).

Conclusions.—We have performed unconstrained simulations of a quantum vortex dynamics in a superfluid neutron medium in the presence of a nucleus using an appropriate time-dependent extension of DFT to a superfluid system. We have determined that the vortex-nucleus force is repulsive and increasing in magnitude with density for the densities characteristic of the neutron star crust (0.014 and 0.031 fm^{-3}). The vortex line shape is strongly affected by the interaction at small separations, leading to significant bending and its lengthening, controlled by the size of the nucleus. Moreover, the vortex-nucleus interaction also induces a deformation of the nucleus. These results demonstrate that the vortex-nucleus interaction cannot be described by a function of their separation alone. To fully characterize the vortex-nucleus interaction, we have extracted the force per unit length for various vortex-nucleus configurations. For velocities of any ambient flow in the background smaller than $v_c \sim (1\text{–}5) \times 10^{-4} c$, the pinned superfluid can store enough angular momentum to drive the giant glitches seen in pulsars [26].

We are grateful to K. J. Roche and A. Sedrakian for helpful discussions and comments. We thank Witold

Rudnicki, Franciszek Rakowski, Maciej Marchwiany and Kajetan Dutka from the Interdisciplinary Centre for Mathematical and Computational Modelling (ICM) of Warsaw University for useful discussions concerning code optimization. This work was supported by the Polish National Science Center (NCN) under Contract No. UMO-2013/08/A/ST3/00708. The method used for generating initial states was developed under a grant of Polish NCN under Contract No. UMO-2014/13/D/ST3/01940. Calculations have been performed at: the resources of the Oak Ridge Leadership Computing Facility (OLCF) Titan, which is a Department of Energy (DOE) Office of Science User Facility supported under Contract No. DE-AC05-00OR22725; the resources of the National Energy Research Scientific computing Center (NERSC) Edison, which is supported by the Office of Science of the U.S. Department of Energy under Contract No. DE-AC02-05CH11231; the resources provided by the Interdisciplinary Computational Science Program in Center for Computational Sciences, University of Tsukuba, HA-PACS (PACS-VIII) system. This work was supported in part by U.S. DOE Office of Science Grant No. DE-FG02-97ER41014, and a Washington State University (WSU) New Faculty Seed Grant.

*gabrielw@if.pw.edu.pl
†sekizawa@if.pw.edu.pl
‡magiersk@if.pw.edu.pl
§bulgac@uw.edu
‖michael.forbes@wsu.edu

[1] V. Radhakrishnan and R. N. Manchester, Detection of a change of state in the pulsar PSR 0833-45, Nature (London) **222**, 228 (1969).
[2] P. E. Reichley and G. S. Downs, Observed decrease in the periods of pulsar PSR 0833-45, Nature (London) **222**, 229 (1969).
[3] J. M. Lattimer and M. Prakash, The physics of neutron stars, Science **304**, 536 (2004).
[4] P. W Anderson and N Itoh, Pulsar glitches and restlessness as a hard superfluidity phenomenon, Nature (London) **256**, 25 (1975).
[5] B. Haskell and A. Melatos, Models of pulsar glitches, Int. J. Mod. Phys. D **24**, 1530008 (2015).
[6] P. M. Pizzochero, L. Viverit, and R. A. Broglia, Vortex-Nucleus Interaction and Pinning Forces in Neutron Stars, Phys. Rev. Lett. **79**, 3347 (1997).
[7] P. Donati and P. M. Pizzochero, Is there Nuclear Pinning of Vortices in Superfluid Pulsars, Phys. Rev. Lett. **90**, 211101 (2003).
[8] P. Donati and P. M. Pizzochero, Realistic energies for vortex pinning in intermediate-density neutron star matter, Phys. Lett. B **640**, 74 (2006).
[9] P. Donati and P. M. Pizzochero, Fully consistent semi-classical treatment of vortexnucleus interaction in rotating neutron stars, Nucl. Phys. **A742**, 363 (2004).
[10] S. Seveso, P. M. Pizzochero, F. Grill, and B. Haskell, Mesoscopic pinning forces in neutron star crusts, Mon. Not. R. Astron. Soc. **455**, 3952 (2016).
[11] P. Avogadro, F. Barranco, R. A. Broglia, and E. Vigezzi, Quantum calculation of vortices in the inner crust of neutron stars, Phys. Rev. C **75**, 012805(R) (2007).
[12] P. Avogadro, F. Barranco, R. A. Broglia, and E. Vigezzi, Vortex-nucleus interaction in the inner crust of neutron stars, Nucl. Phys. **A811**, 378 (2008).
[13] P. M. Pizzochero, Pinning and binding energies for vortices in neutron stars: comments on recent results, arXiv:0711.3393.
[14] S. Jin, A. Bulgac, K. Roche, and G. Wlazłowski, Coordinate-space solver for superfluid many-fermion systems with shifted conjugate orthogonal conjugate gradient method, arXiv:1608.03711.
[15] A. Bulgac, M. M. Forbes, and R. Sharma, Strength of the Vortex-Pinning Interaction from Real-Time Dynamics, Phys. Rev. Lett. **110**, 241102 (2013).
[16] See Supplemental Material at http://link.aps.org/supplemental/10.1103/PhysRevLett.117.232701 for discussion of technical aspects including generation of initial configurations, integration of TDSLDA equations, vortex detection algorithm, force per unit length fitting procedure, and list of accompanying movies, which includes Refs. [17–25].
[17] A. Bulgac, M. M. Forbes, K. J. Roche, and G. Wlazłowski, Quantum friction: Cooling quantum systems with unitary time evolution, arXiv:1305.6891.
[18] R. Takayama, T. Hoshi, T. Sogabe, S.-L. Zhang, and T. Fujiwara, Linear algebraic calculation of Green's function for large-scale electronic structure theory, Phys. Rev. B **73**, 165108 (2006).
[19] S. Yamamoto, T. Sogabe, T. Hoshi, S.-L. Zhang, and T. Fujiwara, Shifted COCG method and its application to double orbital extended Hubbard model, J. Phys. Soc. Jpn. **77**, 114713 (2008).
[20] S. Gandolfi, A. Gezerlis, and J. Carlson, Neutron matter from low to high density, Annu. Rev. Nucl. Part. Sci. **65**, 303 (2015).
[21] H. Lamb, *Hydrodynamics* (Cambridge University Press, Cambridge, England, 1975).
[22] P. Magierski and A. Bulgac, Nuclear hydrodynamics in the inner crust of neutron stars, Acta Phys. Pol. B **35**, 1203 (2004).
[23] P. Magierski, In-medium ion mass renormalization and lattice vibrations in the neutron star crust, Int. J. Mod. Phys. E **13**, 371 (2004).
[24] L. G. Cao, U. Lombardo, and P. Schuck, Screening effects in superfluid nuclear and neutron matter within Brueckner theory, Phys. Rev. C **74**, 064301 (2006).
[25] A. S. Umar, V. E. Oberacker, C. J. Horowitz, P.-G. Reinhard, and J. A. Maruhn, Swelling of nuclei embedded in neutron gas and consequences for fusion, Phys. Rev. C **92**, 025808 (2015).
[26] B. Link, Dynamics of Quantum Vorticity in a Random Potential, Phys. Rev. Lett. **102**, 131101 (2009).
[27] *Quantized Vortex Dynamics and Superfluid Turbulence*, edited by C. F. Barenghi, R. J. Donnelly, and W. F. Vinen, Lecture Notes in Physics (Springer-Verlag, Berlin, 2001), Vol. 571.

[28] R. I. Epstein and G. Baym, Vortex drag and the spin-up time scale for pulsar glitches, Astrophys. J. **387**, 276 (1992).
[29] R. I. Epstein and G. Baym, Vortex pinning in neutron stars, Astrophys. J. **328**, 680 (1988).
[30] M. Antonelli and P. Pizzochero, Axially symmetric equations for differential pulsar rotation with superfluid entrainment, Mon. Not. R. Astron. Soc. **464**, 721 (2017).
[31] A. Bulgac and S. Yoon, Large Amplitude Dynamics of the Pairing Correlations in a Unitary Fermi Gas, Phys. Rev. Lett. **102**, 085302 (2009).
[32] A. Bulgac, Y.-L. Luo, P. Magierski, K. J. Roche, and Y. Yu, Real-time dynamics of quantized vortices in a unitary Fermi superfluid, Science **332**, 1288 (2011).
[33] A. Bulgac, P. Magierski, and M. M. Forbes, The Unitary Fermi Gas: From Monte Carlo to Density Functionals, in *The BCS-BEC Crossover and the Unitary Fermi Gas*, edited by W. Zwerger, Lecture Notes in Physics (Springer, Heidelberg, 2012), Vol. 836, pp. 305–373.
[34] A. Bulgac, Y.-L. Luo, and K. J. Roche, Quantum Shock Waves and Domain Walls in Real-Time Dynamics of a Superfluid Unitary Fermi Gas, Phys. Rev. Lett. **108**, 150401 (2012).
[35] A. Bulgac, Time-dependent density functional theory and real-time dynamics of Fermi superfluids, Annu. Rev. Nucl. Part. Sci. **63**, 97 (2013).
[36] A. Bulgac, M. M. Forbes, M. M. Kelley, K. J. Roche, and G. Wlazłowski, Quantized Superfluid Vortex Rings in the Unitary Fermi Gas, Phys. Rev. Lett. **112**, 025301 (2014).
[37] G. Wlazłowski, A. Bulgac, M. M. Forbes, and K. J. Roche, Life cycle of superfluid vortices and quantum turbulence in the unitary Fermi gas, Phys. Rev. A **91**, 031602(R) (2015).
[38] I. Stetcu, A. Bulgac, P. Magierski, and K. J. Roche, Isovector giant dipole resonance from 3D time-dependent density functional theory for superfluid nuclei, Phys. Rev. C **84**, 051309(R) (2011).
[39] I. Stetcu, C. A. Bertulani, A. Bulgac, P. Magierski, and K. J. Roche, Relativistic Coulomb Excitation within Time-Dependent Superfluid Local Density Approximation, Phys. Rev. Lett. **114**, 012701 (2015).
[40] A. Bulgac, P. Magierski, K. J. Roche, and I. Stetcu, Induced Fission of ^{240}Plutonium within a Real-Time Microscopic Framework, Phys. Rev. Lett. **116**, 122504 (2016).
[41] P. Magierski, Nuclear Reactions and Superfluid Time Dependent Density Functional Theory, in *Progress of Time-Dependent Nuclear Reaction Theory* edited by Y. Iwata, Frontiers in Nuclear and Particle Physics (Bentham Science Publishers, 2016).
[42] J. Negele and D. Vautherin, Neutron star matter at sub-nuclear densities, Nucl. Phys. **A207**, 298 (1973).
[43] S. A. Fayans, Towards a universal nuclear density functional, JETP Lett. **68**, 169 (1998).
[44] S. A. Fayans, S. V. Tolokonnikov, E. L. Trykov, and D. Zawischa, Nuclear isotope shifts within the local energy-density functional approach, Nucl. Phys. **A676**, 49 (2000).
[45] B. Friedman and V. R. Pandharipande, Hot and cold nuclear and neutron matter, Nucl. Phys. **A361**, 502 (1981).
[46] R. B. Wiringa, V. Fiks, and A. Fabrocini, Equation of state for dense nucleon matter, Phys. Rev. C **38**, 1010 (1988).
[47] Y. Yu and A. Bulgac, Energy Density Functional Approach to Superfluid Nuclei, Phys. Rev. Lett. **90**, 222501 (2003) and Appendix to: Energy density functional approach to superfluid nuclei, arXiv:nucl-th/0302007.
[48] S. V. Tolokonnikov, I. N. Borzov, M. Kortelainen, Yu. S. Lutostansky, and E. E. Saperstein, Fayans functional for deformed nuclei. Uranium region, EPJ Web Conf. **107**, 02003 (2016), and earlier references therein.
[49] A. Bulgac and Y.Yu, Spatial Structure of a Vortex in Low Density Neutron Matter, Phys. Rev. Lett. **90**, 161101 (2003).
[50] A. Bulgac and Y. Yu, Renormalization of the Hartree-Fock-Bogoliubov Equations in the Case of a Zero Range Pairing Interaction, Phys. Rev. Lett. **88**, 042504 (2002).
[51] A. Bulgac, Local density approximation for systems with pairing correlations, Phys. Rev. C **65**, 051305(R) (2002).
[52] A. Bulgac and Y. Yu, The Vortex State in a Strongly Coupled Dilute Atomic Fermionic Superfluid, Phys. Rev. Lett. **91**, 190404 (2003).
[53] A. Bulgac, Local density functional theory for superfluid fermionic systems: The unitary gas, Phys. Rev. A **76**, 040502(R) (2007).
[54] A. Bulgac and M. M. Forbes, A Unitary Fermi Supersolid: The Larkin-Ovchinnikov Phase, Phys. Rev. Lett. **101**, 215301 (2008).
[55] A. Sedrakian, Vortex repinning in neutron star crusts, Mon. Not. R. Astron. Soc. **277**, 225 (1995).
[56] M. J. H. Ku, W. Ji, B. Mukherjee, E. Guardado-Sanchez, L. W. Cheuk, T. Yefsah, and M. W. Zwierlein, Motion of a Solitonic Vortex in the BEC-BCS Crossover, Phys. Rev. Lett. **113**, 065301 (2014).
[57] M. J. H. Ku, B. Mukherjee, T. Yefsah, and M. W. Zwierlein, Cascade of Solitonic Excitations in a Superfluid Fermi Gas: From Planar Solitons to Vortex Rings and Lines, Phys. Rev. Lett. **116**, 045304 (2016).
[58] N. Andersson, T. Sidery, and G. L. Comer, Superfluid neutron star turbulence, Mon. Not. R. Astron. Soc. **381**, 747 (2007).
[59] W. F. Vinen and J. J. Niemela, Quantum turbulence, J. Low Temp. Phys. **128**, 167 (2002).
[60] M. Tsubota, M. Kobayashi, and H. Takeuchi, Quantum hydrodynamics, Phys. Rep. **522**, 191 (2013).